EasyChair Preprint

№ 9718

Modeling Thermal Management of Battery Energy Storage System with Machine Learning

Amir Mosavi and F. Kristina

February 15, 2023

Modeling Thermal Management of Battery Energy Storage System with Machine Learning

A. Mosavi, F. Kristina

TU-Dresden, Dresden, Germany
Slovak University of Technology, Bratislava, Slovakia

Abstract

Battery energy storage systems (BESS) are nowadays essential parts of microgrids. A thermal management system (TMS) belongs to substantial control components ensuring optimal operation and long lifespan of batteries. Advanced control strategies implemented in TMS require accurate thermal models to keep battery temperature within predefined bounds while minimizing operating costs. This paper proposes machine learning-based models to predict temperature inside real industrial BESS. Challenges represent partially continuous and partially discrete input signals. Furthermore, inner fans located inside modules affect the temperature in this particular BESS. Unfortunately, the information on fans' operations is not available. This study also provides an accuracy analysis of bagged classification and regression trees (CART), multi-layer perceptron (MLP), and averaged neural network (avNNet). The results report high prediction accuracy, over 95%, for all models, even the ones with a more straightforward structure.

Key words: Thermal management system, Battery energy storage, Modeling, Machine learning.

1 Introduction

Renewable energy sources (RESs), especially solar panels and wind turbines, have become integral to daily life. They are not only operated as a complement to the global grid or in large structures in the industry but also as small-rate systems in households, smart buildings, or public infrastructure. RESs have gained much popularity due to their potential to reduce greenhouse gas emissions, as mentioned in [17]. Since the European Union is committed to decarbonizing its power sector, the study [30] prepared for the European Parliament's Committee on Economic and Industry, Research and Energy (ITRE) suggested that RES, in combination with nuclear plants, should become the primary power sources. Despite the positive impact of RES on the decarbonizing grid, the authors of [6] have pointed out that RESs are accompanied by the problem of the fluctuating amount of produced energy. It results in an insufficient economic operation with a negligible impact on improving the environmental situation.

To overcome these negative aspects and stabilize the operation of the whole grid, energy storage has to be installed in the system. Energy storage is essential to the smooth, economical, and optimal operation of grids and microgrids, as stated in [6]. There are different types of energy storage: thermal, mechanical, electromagnetic, electrochemical (described in more detail in [21]), hydro or compressed air energy storage, and many more summarized by the authors in [6]. The most practical and commonly used energy storage system is a battery energy storage system (BESS). Lithium-based BESS has been proved to be the most effective due to its high efficiency, high energy density, and long lifetime, as stated and graphically illustrated in the work of [23].

To ensure the safe and smooth operation of BESS, the energy management system (EMS) and thermal management system (TMS) must be properly configured. EMS has been studied with meticulous care over the past decade, and a lot of approaches can be found in the literature from different perspectives like [10], [20], [11], [22] just to name a few. The TMS development lags behind that of EMS due to the low importance in grid operation (compared to EMS). However, TMS is closely related to the economic view of grid/microgrid operation. It has been proven in [19] that if the battery temperature increases by 1°C in the range $30 - 40$°C, the battery lifespan is reduced by two months. Furthermore, high battery temperature can lead to accelerated capacity fade, aging, and damnification following environmental problems as studied by the authors in [26]. On the other hand, the work of [12] shows that low battery temperature reduces power capability or performance failure. It implies that unsuitable thermal management of BESS affects the operation of EMS. The optimal range for battery temperature deviates from one study to another. In [8], the acceptable range is between -20 $-$ 60°C, in [18] the optimal temperature range for lithium-based batteries is $15 - 35$°C. Generally, in industry, the acceptable

range is defined by the manufacturer.

Although TMS is inconspicuous, it is crucial for optimal BESS performance. Different control strategies have been employed to ensure an adequate temperature in BESS. The PID controller for regulating the thermal balance of the stack in hybrid vehicles was proposed in [29]. It was shown that the PID controller could stabilize the stack's temperature even with low cooling water flow at the cost of a higher fan and pumping power. The authors of [16] introduced a novel fuzzy control strategy to maintain a suitable battery temperature range in electric vehicles. It has been verified that this strategy can extend the battery lifetime. However, the specific influence on the battery pack has not been investigated further. PID and fuzzy controllers are practical due to straightforward design, implementation, and tuning. Nevertheless, it isn't easy to achieve BESS's economic operation, considering the environmental impact of these two types of control strategies.

Therefore, the model predictive control (MPC) strategy plays a crucial role in the energy sector, including battery thermal management. The authors of [13] proposed a nonlinear model predictive controller (NMPC) method to optimize the cooling process of batteries in electric vehicles. The study reports performance comparisons of NMPC and PID controllers, concluding that NMPC is preferable due to reduced coolant consumption, reduced inconsistency of the battery module temperature, and precise reference tracking. On the other hand, the computational time of NMPC is 50-times higher than for PID. However, it is still sufficient. Another implementation of MPC can be found in [15], [25], [28], and many more. Even though these strategies were mostly applied in electric vehicle research, they can be modified and implemented in BESS thermal control management.

As the name suggests, the model of the controlled process is essential for the MPC strategy. The control performance of MPC depends on the precision of the model. In the process control perspective, the state-space models are preferred over nonlinear or complicated models. Identification of the state-space battery thermal model can be found in [5], where the authors constructed the state-space model using step response obtained from the computational fluid dynamics (CFD) model. A state-space-based multi-nodes thermal model can be found in [27], where the model is derived from battery heat transfer process equations. Both methods require detailed knowledge about the thermal behavior of particular BESS. Furthermore, CDF analysis can be costly. The heat transfer process equations models require perfect knowledge about the system and thermodynamic laws. Therefore, the identification from real-time data can represent an appropriate alternative. However, the drawback is the demand for a considerable amount of data.

The studies mentioned above operate with analytical mathematical models of battery thermal behavior. Another approach is to estimate battery temperature using recurrent neural networks as presented in [9]. However, this model was identified for monitoring purposes and was trained and validated on a dataset acquired from NASA's Prognostics Center of Excellence (PCoE). The authors illustrated a similar idea in [7] using artificial neural networks. The data used for training and validation were extracted from [14], where they were obtained from an experimental laboratory device.

This paper presents several machine learning modeling techniques used to approximate the thermal behavior of industrial battery energy storage based on real-time data. Compared with previous work, we analyze temperature evolution in a rack containing multiple battery modules, where each performs differently. Moreover, the models presented in this paper handle combination of continuous and discrete input variables. Additionally, the BESS has been designed with features such as inner fans influencing the battery temperatures, but the information about the fans' operation is unavailable. Nevertheless, despite the mentioned obstacles, we can obtain a BESS thermal model that precisely predicts temperature evolution inside the rack.

2 Materials

This section introduces our studied system, its current implementation, and particular features influencing output variables.

2.1 Studied System

The industrial BESS studied in this paper is located in Liptovský Hrádok, Slovakia, and installed as a part of the microgrid. It is adapted to store the spare energy from solar panels or the grid during low-price periods. In addition, the BESS energy is used for peak-shaving or to prevent deviations from the reported day-ahead diagram. The microgrid structure is illustrated in Fig. 1. The BESS is composed of 3 parts: the battery part, heating, ventilation, and cooling (HVAC) part, and inverter part. The first section contains ten lithium-ion battery modules with NMC (nickel-mangan-cobalt) cathode. Altogether, they create BESS with a battery capacity of around 150 kWh. During the charging or discharging process, the modules emit a certain amount of heat, which can vary between modules. The battery part also disposes of a ventilation fan situated at the top of the rack. The fan provides air exchange between BESS and its surroundings and operates in a continuous regime. The air is drawn in from below the BESS and is vented out at the top. The HVAC module contains an air conditioning (AC) unit, which can operate in two modes: cooling or heating. Adjusted air enters the bottom of

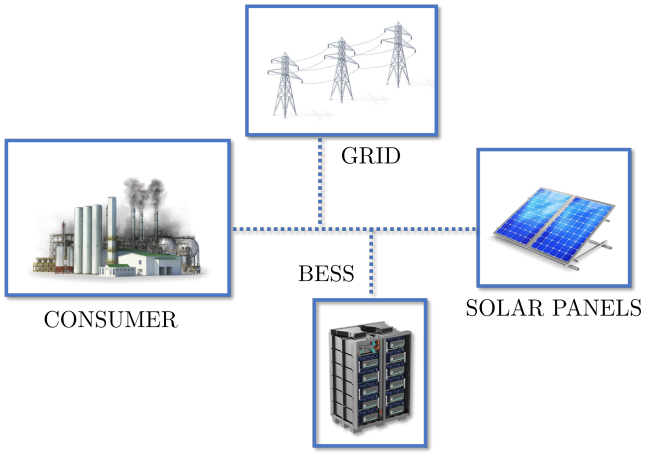

Fig. 1. The illustration of microgrid structure. The BESS can be charged by power from solar panels or a grid. On the other hand, battery power is used to fulfill consumer requirements while minimizing deviations and costs.

the battery part and returns to the HVAC part through the circulation fan at the top. All HVAC features can be only in active or inactive mode introducing discrete variables to our system. The inverter part is essential for the energy management system. However, it is isolated from the rest of BESS. Therefore its thermal impact on the battery temperature is negligible. The BESS structure and air flows are illustrated in Fig. 2. Note that battery modules have build-in fans whose operation cannot be monitored. Furthermore, no thermal model has been found yet.

2.2 Current Implementation

Since the BESS is currently operational, it is already accompanied by the thermal management system. It represents a rule-based controller, which collects ambient and BESS temperature measurements to produce commands for HVAC and fans based on a set of rules as portrayed in Fig. 6. It is an effortless but acceptable control. Generally, the rule-based and PID controllers are primarily used in the TMS of industrial batteries. The problem is not the implementation of advanced control strategies but the complexity of obtaining the appropriate thermal model. However, HVAC operation is not optimized to achieve economic goals. Moreover, if the BESS is in the process of charging or discharging, it is detected by TMS when temperature measurements are collected. Therefore, it results in delayed cooling, which leads to a violation of the optimal temperature range. The thermal range for this particular BESS is shown in Fig. 3 with temperature impact on maximal battery power rate. The gray area represents the suitable range defined by the manufacturer when the battery power output is maximized. However, the interval is shrunken (green area) for safety and stable operation. Last but not least, using a rule-based controller generates a maximum difference of

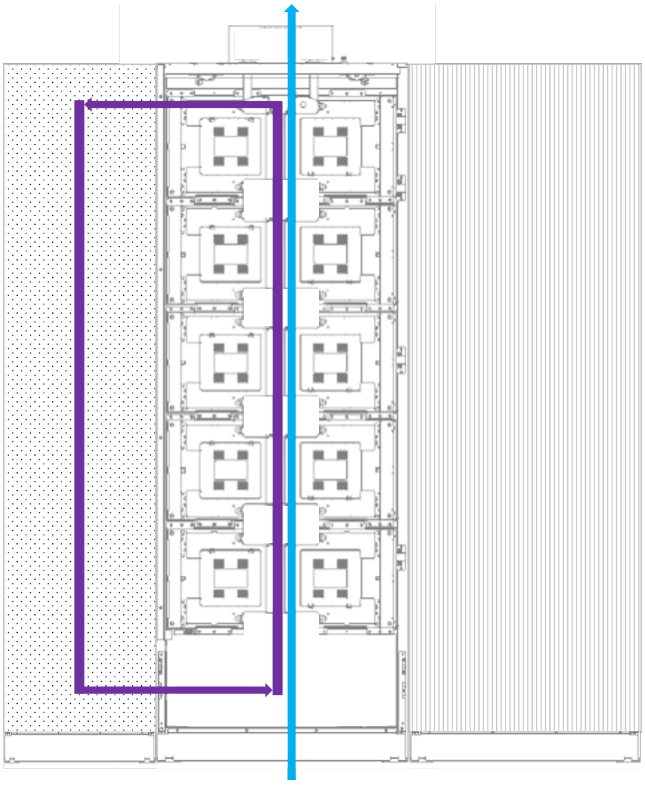

Fig. 2. The structure of BESS: the left dotted part represents HVAC, the middle part is the battery part composed of battery modules, and the right dashed part contains the inverter. The blue arrow illustrates air flow through BESS generated by the battery ventilation fan. The purple arrows represent air circulation between batteries and HVAC.

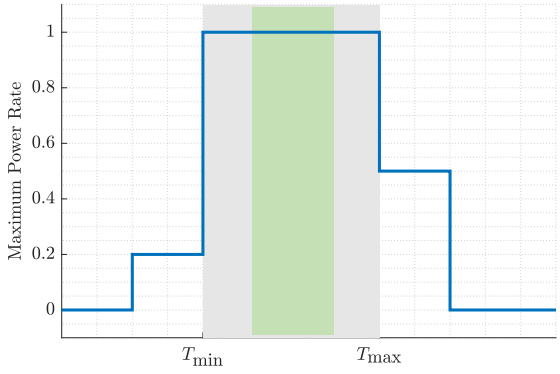

Fig. 3. The dependence of maximum power rate on temperature. The optimal operation conditions are between $T_{\min}$ and $T_{\max}$ (gray area), because that is when we work with maximum battery power. The green area represents the interval considered by the controller for safety and stability.

9.8°C between a minimum and maximum temperatures in BESS, which is undesirable.

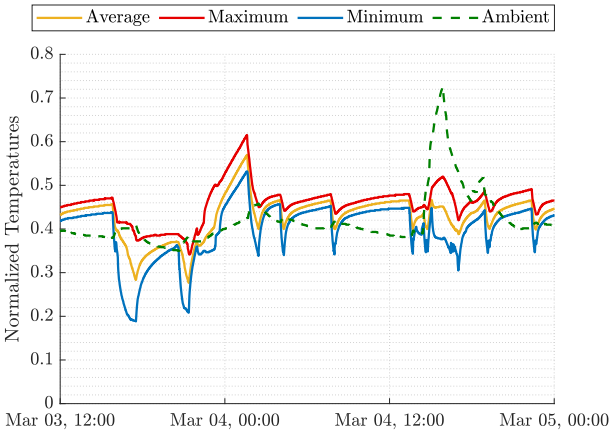

Fig. 4. Evolution of temperatures in battery part of BESS. The enormous temperature changes are caused by intentional step tests, where the impact of HVAC features was investigated in detail. The ambient temperature increased its value on March 4th at 16:00 due to a colossal heat exchange between BESS and its surroundings.

2.3 Dataset

Our dataset for identification and validation is created from data measured in the battery energy storage system, which are collected in real-time. Measurements are stored in the database with 1 minute sampling time. Since our industrial partner does not wish to share exact values of variables, we applied so-called min-max normalization to overcome this issue. The general formula is defined as

$$x = \frac{x_{\text{org}} - x_{\min}}{x_{\max} - x_{\min}}, \tag{1}$$

where x_{org} is original measured value of variable, $x_{\min}$ and $x_{\max}$ are normalization limits and $x \in [0, 1]$ is normalized value.

As we already know, the temperature of BESS modules is influenced by the operation of HVAC, ambient temperature, and the amount of charged/discharged energy to/from the module since charging and discharging the battery emits heat. The temperatures considered as our system's outputs are the average $T^{\text{BAT}}_{\text{avg}}$, minimal $T^{\text{BAT}}_{\text{min}}$, and maximal $T^{\text{BAT}}_{\text{max}}$ temperatures of modules in battery part. These signals describe the thermal behavior of BESS because they directly influence the length of battery lifespan and value of maximal charged/discharged power, therefore the economic aspect of BESS operation. Furthermore, these signals are essential for controller design. The first four BESS inputs represent the cooling u_{C} and heating u_{H} of modules using the HVAC system, circulation fan u_{CF} used for distribution of cooled/heated air from HVAC part to battery part, and ventilation fan u_{F} used for passive cooling. These signals are controlled by a thermal management system (TMS). Other input signals are charging and discharging battery power al-

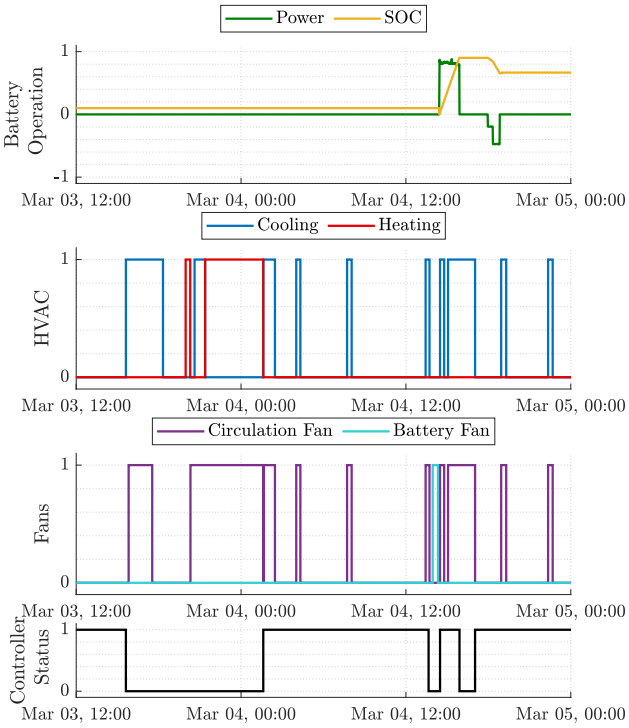

Fig. 5. Evolution of control inputs in battery part of BESS. When the controller status is equal to 1, the TMS is running, meaning that the rule-based controller produces appropriate control actions. If controller status is 0, the actuators are manually controlled, representing step tests.

together P_{S} and ambient temperature T_{amb}. TMS cannot control them, considering the ambient temperature depends on the location of BESS as much as the conditions near BESS, and the amount of charged or discharged power is defined by the energy management system (EMS). The EMS is prioritized over TMS since it ensures the safe and smooth operation of the whole microgrid. Therefore P_{S} and T_{amb} are considered as disturbances. However, we can model their impact on the modules' temperatures. Fig. 4 illustrates measured output and ambient temperatures over 1.5 days period. The belonging control actions are portrayed in Fig. 5 to clarify the impact of HVAC and fans operation on BESS temperatures. Since the BESS is already operational with active TMS, the dataset is partially composed of temperature data, measured when the controller was active, and data without any temperature control representing our step tests. Parameter C_{aut} in Fig. 5 represents the information about status of controller. If $C_{\text{aut}} = 1$, the controller was active (on), if $C_{\text{aut}} = 0$, thermal control was off.

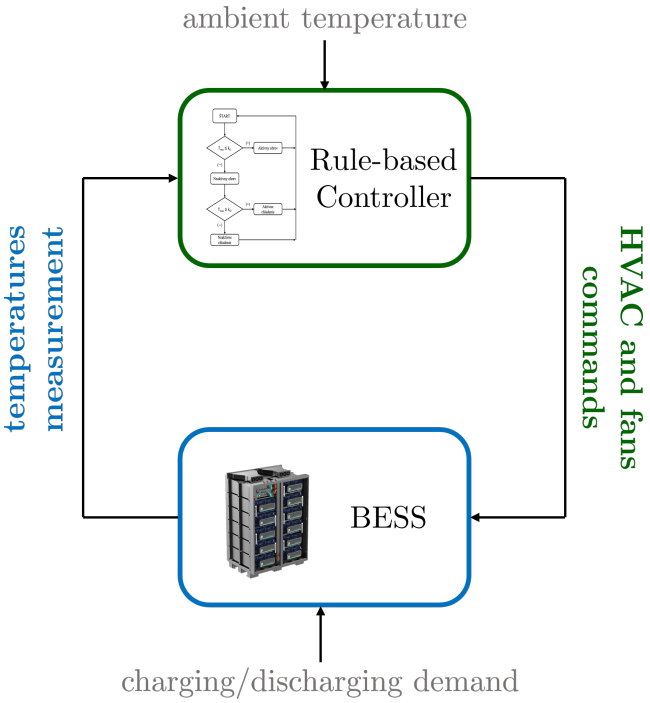

Fig. 6. The closed-loop system: rule-based controller produces control actions (command for HVAC and fans) based on ambient temperature and temperature measurements from BESS. The thermal conditions in BESS are not only influenced by mentioned controlled actions but also by the demand on battery power, which the controller has no knowledge about.

3 Methods

This section describes three machine learning strategies that have reported the best results in modeling BESS temperature.

3.1 Bagged Classification and Regression Trees

The classification and regression trees (CART), historically called decision trees, are a statistical and predictive modeling method introduced by Breiman et al. in [3]. The classification tree algorithm decides which of the predefined classes the target value most likely belongs. The regression tree refers to an algorithm that predicts the value of a continuous target variable. The data set in the CART method is partitioned into multiple subsets, each representing one branch. Then, the model is obtained by applying the recursive segmentation technology within each partition. Gained set of rules is used to predict the target variable. The advantages of this modeling approach are the model's simplicity and negating the need for linearity assumptions. Furthermore, the CART model can operate with both discrete and continuous variables. On the other hand, using CART models can create a problem such as overfitting, high variance, and low bias.

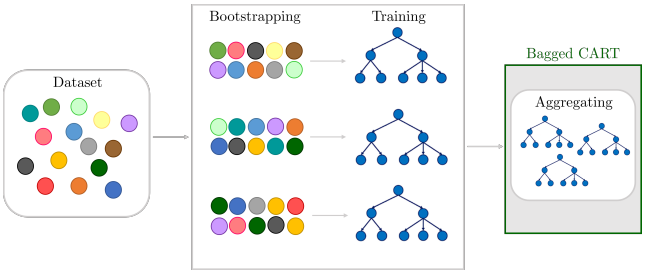

Fig. 7. Visualization of algorithm generating bagged CART model. Each circle represents the input instance. After finding the bagged CART model, the testing data are inserted in each decision tree inside the model and obtained outputs are averaged, creating a target value.

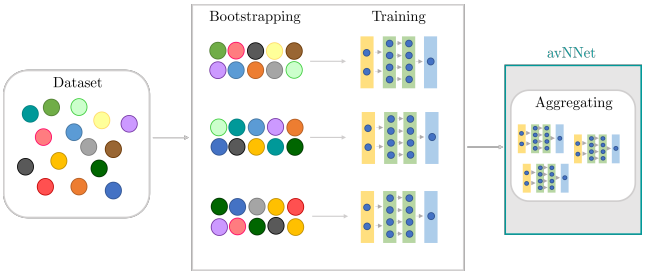

Fig. 8. Visualization of avNNet model. Like bagged CART, several randomized subsets of the original dataset are used to train multiple ANNs. The value of the target variable is obtained as an average of all ANNs outputs.

Since the CART is considered sensitive to the trained data, it reports high prediction variance for other input data. Bootstrap Aggregation (Bagging) is an ensemble method used to increase the prediction accuracy of the CART model. The bagged CART method is the procedure where multiple CART models are trained using random subsets of our original dataset. The target value is calculated as an average of the models' outputs. Bagged Cart has been proved to be an efficient strategy to improve accuracy as stated in [2].

3.2 Multi-Layer Perceptron

The multi-layer perceptron (MLP) is a classic fully connected feed-forward artificial neural network (ANN) consisting of one input, multiple hidden, and one output layer. The layers contain several nodes called neurons. The number of neurons in the input and output layer equals the number of inputs and outputs in the dataset. The number of hidden layers and nodes within it can be chosen. All neurons are connected in a feed-forward fashion, and their inputs are weighted. These inputs are summed up inside each neuron, and subsequently, a bias parameter specific for each neuron is added to the result. The outcome is converted to node output using the selected activation function. The MLP uses the backpropagation algorithm to adjust the weights and biases to minimize the difference between outputs from the dataset and predicted values from the MLP model. The

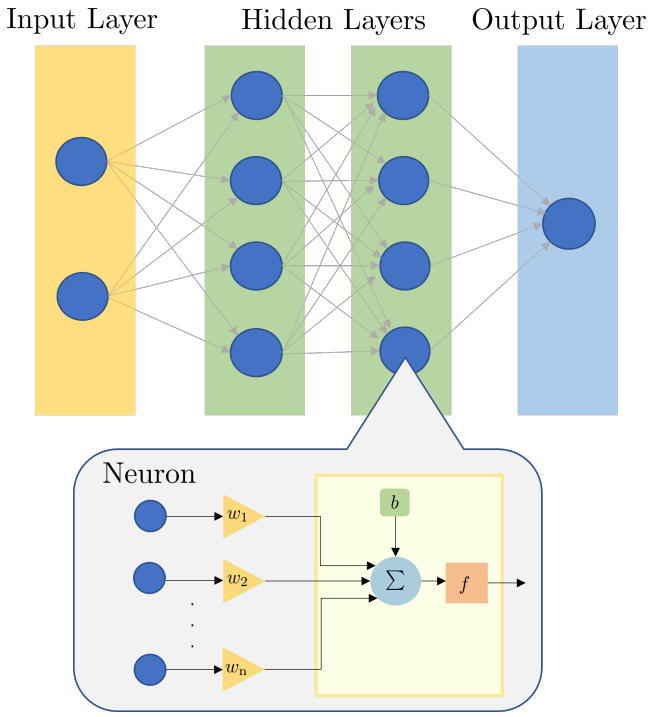

Fig. 9. Visualization of MLP model. The input variables are modified multiple times as they are transported through the network in a feed-forward fashion. They are weighted, added up, and transformed using the activation function in neurons to produce the final output. The results are compared to the expected value, and based on the deviation size, the backpropagation algorithm takes charge.

authors of [1] declare that the presented method applies to complex nonlinear systems even with extensive input data and gains high accuracy ratio if adequately set.

3.3 Averaged Neural Network

The averaged neural network (avNNet) model represents a combination of bagged CART and MLP features. It is created by training multiple artificial neural networks with the same structure on random seeds of data from the original dataset. The target values are obtained by averaging the outputs from all neural networks in the avNNet. Since the ANNs are trained using different subsets, they can differ in values of parameters. The benefits of using the avNNet are that the network ensemble can be far less fallible than one network, as discussed and experimentally shown in [4]. Furthermore, avNNet reports a high possibility of over-fitting and over-training avoidance as stated in [24].

3.4 Model Quality

To compare the presented models, we have chosen four quality parameters. The first one is Root Mean Squared Error (RMSE). This criterion aggregates the squared magnitudes of errors between measured output y and predicted value $\hat{y}$. The mathematical formula of RMSE is defined as

$$\mathrm{RMSE} = \sqrt{\frac{\sum_{k=1}^{N}(\hat{y}_k - y_k)^2}{N}}. \tag{2}$$

The second criterion is Mean Absolute Error (MAE), which operates with an absolute difference between y and $\hat{y}$. It is formulated as follows

$$\mathrm{MAE} = \frac{\sum_{k=1}^{N}|\hat{y}_k - y_k|}{N}. \tag{3}$$

Both RMSE and MAE are parameters describing the accuracy of modeling. However, the RMSE parameter is more helpful in considering undesirable large errors because it squared the errors before averaging. The coefficient of determination, denoted as R^2, is the third quality parameter representing the closeness of data to the fitted regression line. It is evaluated as

$$R^2 = 1 - \frac{\sum_{k=1}^{N}(\hat{y}_k - y_k)^2}{\sum_{k=1}^{N}(y_k - \overline{y})^2}, \tag{4}$$

where $\overline{y}$ is the mean of measured outputs y. From the definition $R^2 \in [0, 1]$, where $R^2 = 0$ represents no relationship between y and $\hat{y}$, while $R^2 = 1$ correspond to ideal situation where $y = \hat{y}$. Therefore, higher R^2 symbolizes high prediction accuracy.

4 Results

For this paper, we focused on modeling average BESS temperature. Dynamical models produced by bagged CART, MLP, and avNNet methods consider cooling, heating, circulation fan, ventilation fan, battery power, and ambient temperature as input signals. The dataset in the training phase was constructed from 49,705 samples corresponding to approximately 35 days of data. The models were validated and tested on 21,295 data samples, which is almost 15 days of measurements. The testing phase results are summarized in Tab. 1. As we can see, each model reports high accuracy. However, avNNet declares the lowest RMSE and MAE combined with the highest d and R^2. Fig. 10 illustrates temperature profiles generated from original data and from each model over 600 minutes showing that MLP and the avNNet are very precise in predictions. The operation of inner fans can affect the accuracy of trained models. The ventilators work independently of the TMS, they affect the temperature, but we do not dispose of information about their activity.

Table 1
Summary of quality parameters for bagged CART, MLP, and avNNet models.

Method	RMSE	MAE	d	R^2
Bagged CART	0.011	0.008	0.989	0.958
MLP	0.008	0.007	0.995	0.979
avNNet	0.007	0.006	0.996	0.985

Even though bagged CART reports worse results than the rest, it still provides a model with an accuracy of over 95%. Moreover, the bagged CART model possesses a simple structure, which is exceptionally beneficial in the control design field. The results portrayed in Fig. 11 reports that even though the MLP model produces the lowest value of maximum absolute error, the average difference is the highest compared to other methods.

5 Conclusions

The proposed paper analyzes three machine learning-based models' accuracy, namely bagged CART, MLP, and avNNet, to predict temperature inside BESS. The results show that avNNet declares higher quality performance, even though the accuracy of every model is over 95%. However, under some particular operational conditions, the worst model (bagged CART) has deviated from the original dataset by an immense 3°C. The reason is the BESS containing fans, the operation of which cannot be monitored. They affect the temperature, but we do not dispose of the associated signal. The solution could be the implementation of non-intrusive load monitoring. Another issue represents undetected measurement failures when HVAC features and fans are running, but information about temperature is not logged in the database. After communication is restored, data between these two instances are approximated using interpolation. This problem could be solved by including an anomaly detection algorithm in our system. However, the thermal profiles of presented models report high accuracy. They can be used in advanced control strategies or as a base for deriving linear models. The machine learning models with declared precision are frequently used for monitoring purposes or as digital twins for simulations.

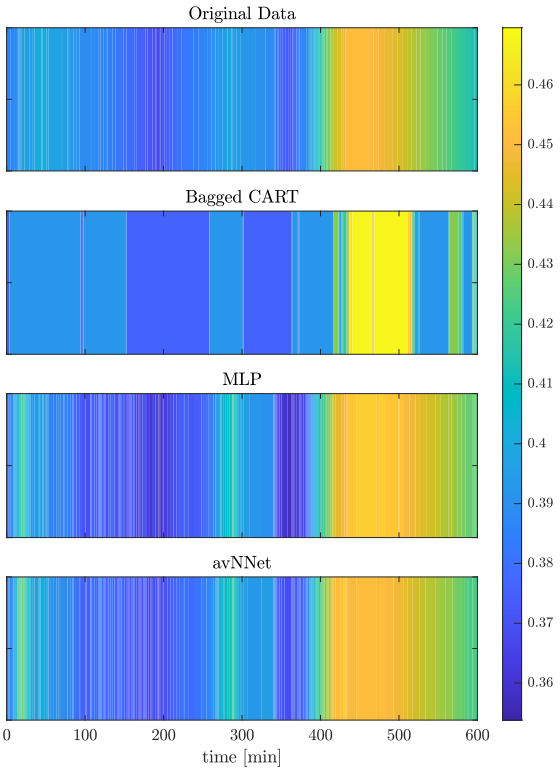

Fig. 10. Comparison of temperature profiles provided by bagged CART, MLP, and avNNet models with original profile extracted from testing dataset. The colorbar on the right side defines the colors belonging to certain normalized temperatures (lowest are represented as dark blue, highest as yellow).

References

[1] B. Akkaya and N. Çolakoğlu. Comparison of multi-class classification algorithms on early diagnosis of heart diseases. In *y-BIS 2019 Conference: ISBIS Young Business and Industrial Statisticians Workshop on Recent Advances in Data Science and Business Analytics*, 09 2019.

[2] L. Breiman. Bagging predictors. *Mach Learn*, 24:123–140, 1994.

[3] L. Breiman, J. Friedman, C.J. Stone, and R.A. Olshen. *Classification and Regression Trees*. Chapman and Hall/CRC, 1984.

[4] L.K. Hansen and P. Salamon. Neural network ensembles. *IEEE Transactions on Pattern Analysis and Machine Intelligence*, 12(10):993–1001, 1990.

[5] X. Hu, L. Chaudhari, S. Lin, S. Stanton, S. Asgari, and W. Lian. A state space thermal model for hev/ev battery using vector fitting. In *2012 IEEE Transportation Electrification Conference and Expo (ITEC)*, pages 1–8, 2012.

[6] H. Ibrahim, A. Ilinca, and J. Perron. Energy storage systems—characteristics and comparisons. *Renewable and Sustainable Energy Reviews*, 12(5):1221–1250, 2008.

[7] F. Jaliliantabar, R. Mamat, and S. Kumarasamy. Prediction of lithium-ion battery temperature in

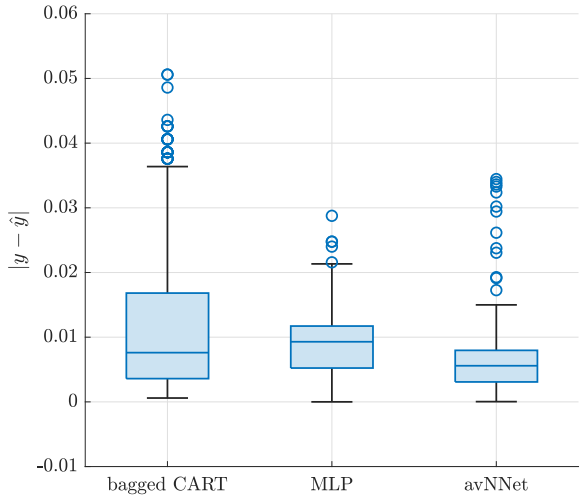

Fig. 11. Statistical representation of absolute error between predicted value and measurement. The circles represent values with the minimum occurrence but a high deviation from average.

different operating conditions equipped with passive battery thermal management system by artificial neural networks. *Materials Today: Proceedings*, 48:1796–1804, 2022. Innovative Manufacturing, Mechatronics & Materials Forum 2021.

[8] Y. Ji, Y. Zhang, and Ch. Wang. Li-ion cell operation at low temperatures. *Journal of the Electrochemical Society*, 160(4):A636–A649, 2013. Cited by: 345.

[9] Y. Jiang, Y. Yu, J. Huang, W. Cai, and J. Marco. Li-ion battery temperature estimation based on recurrent neural networks. *Science China Technological Sciences*, 64, 04 2021.

[10] S. Leonori, E. De Santis, A. Rizzi, and F.M.F. Mascioli. Optimization of a microgrid energy management system based on a fuzzy logic controller. In *IECON 2016 - 42nd Annual Conference of the IEEE Industrial Electronics Society*, pages 6615–6620, 2016.

[11] X. Li and S. Wang. Energy management and operational control methods for grid battery energy storage systems. *CSEE Journal of Power and Energy Systems*, 7(5):1026–1040, 2021.

[12] S. Ma, M. Jiang, P. Tao, Ch. Song, J. Wu, J. Wang, T. Deng, and W. Shang. Temperature effect and thermal impact in lithium-ion batteries: A review. *Progress in Natural Science: Materials International*, 28(6):653–666, 2018.

[13] Y. Ma, H. Ding, H. Mou, and J. Gao. Battery thermal management strategy for electric vehicles based on nonlinear model predictive control. *Measurement*, 186:110115, 2021.

[14] M. Malik, I. Dincer, M. Rosen, and M. Fowler. Experimental investigation of a new passive thermal management system for a li-ion battery pack using phase change composite material. *Electrochimica Acta*, 257:345–355, 2017.

[15] Y. Masoudi and N. L. Azad. Mpc-based battery thermal management controller for plug-in hybrid electric vehicles. In *2017 American Control Conference (ACC)*, pages 4365–4370, 2017.

[16] H. Min, Z. Zhang, W. Sun, Z. Min, Y. Yu, and B. Wang. A thermal management system control strategy for electric vehicles under low-temperature driving conditions considering battery lifetime. *Applied Thermal Engineering*, 181:115944, 2020.

[17] P. Owusu and S. Asumadu Sarkodie. A review of renewable energy sources, sustainability issues and climate change mitigation. *Cogent Engineering*, 3:1167990, 04 2016.

[18] A. Pesaran, S. Santhanagopalan, and G.H. Kim. Addressing the impact of temperature extremes on large format li-ion batteries for vehicle applications (presentation). 2013.

[19] Z. Rao and S. Wang. A review of power battery thermal energy management. *Renewable and Sustainable Energy Reviews*, 15(9):4554–4571, 2011.

[20] E. Reihani, S. Sepasi, L. R. Roose, and M. Matsuura. Energy management at the distribution grid using a battery energy storage system (bess). *International Journal of Electrical Power & Energy Systems*, 77:337–344, 2016.

[21] A. H. Robert. *Energy Storage: Fundamentals, Materials and Applications*. Spinger, 2016.

[22] H. Shafique, L. B. Tjernberg, D.E. Archer, and S. Wingstedt. Energy management system (ems) of battery energy storage system (bess) – providing ancillary services. In *2021 IEEE Madrid PowerTech*, pages 1–6, 2021.

[23] M. Stecca, L. R. Elizondo, T. B. Soeiro, P. Bauer, and P. Palensky. A comprehensive review of the integration of battery energy storage systems into distribution networks. *IEEE Open Journal of the Industrial Electronics Society*, 1:46–65, 2020.

[24] I. V. Tetko, D. J. Livingstone, and A. I. Luik. Neural network studies. 1. comparison of overfitting and overtraining. *Journal of Chemical Information and Computer Sciences*, 35(5):826–833, 1995.

[25] H. Wang, Y. Meng, Q. Zhang, M. R. Amini, I. Kolmanovsky, J. Sun, and M. Jennings. Mpc-based precision cooling strategy (pcs) for efficient thermal management of automotive air conditioning system. In *2019 IEEE Conference on Control Technology and Applications (CCTA)*, pages 573–578, 2019.

[26] R.B Wright, J.P Christophersen, C.G Motloch, J.R Belt, C.D Ho, V.S Battaglia, J.A Barnes, T.Q Duong, and R.A Sutula. Power fade and capacity fade resulting from cycle-life testing of advanced technology development program lithium-ion batteries. *Journal of Power Sources*, 119-121:865–869, 2003. Selected papers presented at the 11th International Meeting on Lithium Batteries.

[27] Y. Xiao and B. Fahimi. State-space based multinodes thermal model for lithium-ion battery. In

2014 IEEE Transportation Electrification Conference and Expo (ITEC), pages 1–7, 2014.

[28] Y. Xie, Ch. Wang, X. Hu, X. Lin, Y. Zhang, and W. Li. An mpc-based control strategy for electric vehicle battery cooling considering energy saving and battery lifespan. *IEEE Transactions on Vehicular Technology*, 69(12):14657–14673, 2020.

[29] L. Xing, W. Xiang, R. Zhu, and Z. Tu. Modeling and thermal management of proton exchange membrane fuel cell for fuel cell/battery hybrid automotive vehicle. *International Journal of Hydrogen Energy*, 47(3):1888–1900, 2022.

[30] G. Zachmann, F. Holz, A. Roth, B. McWilliams, R. Sogalla, F. Meißner, and C. Kemfert. Decarbonisation of energy: Determining a robust mix of energy carriers for a carbon-neutral eu. DIW Berlin: Politikberatung kompakt 175, Berlin, 2021.